Modulation of the Nogo signaling pathway to overcome amyloid-β-mediated neurite inhibition in human pluripotent stem cell–derived neurites

Kirsty Goncalves[1], Stefan Przyborski[1, 2, *]

https://doi.org/10.4103/NRR.NRR-D-23-01628

Date of submission: September 27, 2023

Date of decision: May 29, 2024

Date of acceptance: July 9, 2024

Date of web publication: July 29, 2024

From the Contents

Graphical Abstract

Application of tissue culture models to investigate the involvement of the Nogo signalling pathway in neurite inhibition

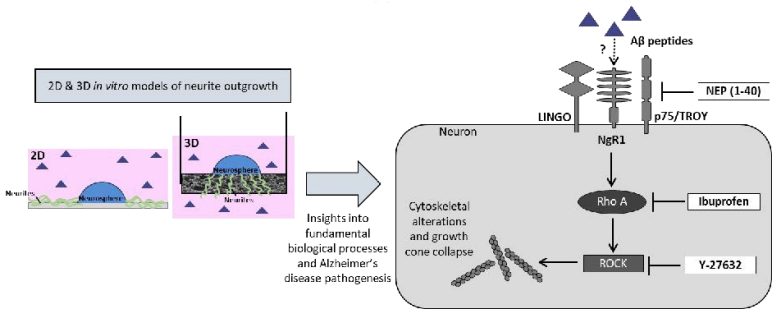

Abstract

Neuronal cell death and the loss of connectivity are two of the primary pathological mechanisms underlying Alzheimer's disease. The accumulation of amyloid-β peptides, a key hallmark of Alzheimer's disease, is believed to induce neuritic abnormalities, including reduced growth, extension, and abnormal growth cone morphology, all of which contribute to decreased connectivity. However, the precise cellular and molecular mechanisms governing this response remain unknown. In this study, we used an innovative approach to demonstrate the effect of amyloid-β on neurite dynamics in both two-dimensional and three-dimensional culture systems, in order to provide more physiologically relevant culture geometry. We utilized various methodologies, including the addition of exogenous amyloid-β peptides to the culture medium, growth substrate coating, and the utilization of human-induced pluripotent stem cell technology, to investigate the effect of endogenous amyloid-β secretion on neurite outgrowth, thus paving the way for potential future applications in personalized medicine. Additionally, we also explore the involvement of the Nogo signaling cascade in amyloid-β-induced neurite inhibition. We demonstrate that inhibition of downstream ROCK and RhoA components of the Nogo signaling pathway, achieved through modulation with Y-27632 (a ROCK inhibitor) and Ibuprofen (a Rho A inhibitor), respectively, can restore and even enhance neuronal connectivity in the presence of amyloid-β. In summary, this study not only presents a novel culture approach that offers insights into the biological process of neurite growth and inhibition, but also proposes a specific mechanism for reduced neural connectivity in the presence of amyloid-β peptides, along with potential intervention points to restore neurite growth. Thereby, we aim to establish a culture system that has the potential to serve as an assay for measuring preclinical, predictive outcomes of drugs and their ability to promote neurite outgrowth, both generally and in a patient-specific manner.

Key Words: Alzheimer's disease; induced pluripotent stem cell; neurite outgrowth; neuron; Nogo; Rho A; ROCK; stem cell; three-dimensional culture

Introduction

Alzheimer's disease (AD), a common neurodegenerative disease, leads to progressive memory loss and functional decline (Kumar et al., 2015). AD symptoms reduce life expectancy and quality of life and result in physical disability. This places a burden not only on those affected and their families but also economically due to an aging population (Sadigh-Eteghad et al., 2015). One of the most widely recognized pathological hallmarks of AD is the extracellular accumulation of aggregated amyloid-β (Aβ) in senile plaques (Murphy and LeVine, 2010; Kumar et al., 2015).

Aberrant processing of amyloid precursor protein gives rise to two major Aβ peptides: $Aβ_{40}$ and $Aβ_{42}$ (Zhang et al., 2011). The longer $Aβ_{42}$ readily forms insoluble fibrils and is more closely linked to AD pathogenesis (Zhang et al., 2011). Elevated levels of $Aβ_{42}$ relative to $Aβ_{40}$ are critical for disease pathogenesis and even considered diagnostic (Spies et al., 2010; Dumurgier et al., 2015; Lewczuk et al., 2015). As neurites pass through senile plaques, they lose their characteristic morphology and retract, disrupting signal transduction, which contributes to memory loss (Jin et al., 2011; Serrano-Pozo et al., 2011). Dendritic abnormalities have been identified in the brains

[1]Department of Biosciences, Durham University, Durham, UK; [2]Reprocell Europe Ltd., Glasgow, UK
***Correspondence to:** Stefan Przyborski, PhD, stefan.przyborski@durham.ac.uk.
https://orcid.org/0000-0001-7613-525X (Stefan Przyborski)

Funding: *This study was supported by a BBSRC CASE training studentship, No. BB/K011413/1 (to KG).*
How to cite this article: *Goncalves K, Przyborski S (2025) Modulation of the Nogo signaling pathway to overcome amyloid-β-mediated neurite inhibition in human pluripotent stem cell–derived neurites. Neural Regen Res 20(9):2645-2654.*

of AD patients, including spine loss, shaft atrophy, bending, branch breaking, and sprouting (Grutzendler et al., 2007), which have been recapitulated *in vitro* through the application of Aβ species to cell-based model systems (Jin et al., 2011). This reduction in connectivity as a consequence of Aβ-deposition and neurite inhibition is thought to contribute to a reduction in plasticity, signal transduction, and even cell-cell communication via synapses (Knowles et al., 1999). This, in combination with other pathogenic mechanisms, is thought to contribute to memory loss, functional decline, and disease progression, despite the underlying molecular mechanisms remaining relatively unknown.

In this study, we combined several advanced *in vitro* techniques to provide insights into the biological mechanism that governs Aβ-mediated neurite inhibition. These include methods of exogenous Aβ peptide presentation, a 3D culture system, and multiple stem cell technologies to demonstrate the extent of Aβ's impact on neurite extension. We utilized both a well-established neurite outgrowth methodology based on a robust model of neural differentiation from embryonal carcinoma cells, and induced pluripotent stem cell (iPSC)-derived neuroprogenitor cells that allow for the patient or disease-specific studies. Through this combination of innovative technologies, we aim to understand the cellular impact of Aβ on neurite dynamics by both a simplistic, reductionist approach and through increasing complexity and physiological relevance. This has allowed us to demonstrate the inhibitory capacity of both $A\beta_{40}$ and $A\beta_{42}$ alone and in combination.

The platform upon which this investigation is built is a well-characterized model system involving differentiation and neurite outgrowth from a well-established embryonal carcinoma cell line (Clarke et al., 2017). This robust, reproducible, and quantifiable model of neurite outgrowth has been applied to many other investigations, such as glial scar-mediated neurite inhibition (Clarke et al., 2017) and the role of extracellular matrix (ECM) motifs in neurite development (Goncalves et al., 2023). To advance this study and re-create a more physiologically relevant system capable of endogenous Aβ production, we also applied this methodology to iPSC-derived neuroprogenitor cells that express a mutation in Presenilin-1 (PSEN1), an enzyme involved in amyloidogenic processing (Cai et al., 2015).

These two novel platforms have provided tools that have allowed us to probe the molecular pathways that govern Aβ-mediated neurite inhibition. The aim was to establish a link between Nogo-receptor activation (a formidable step in glial scar-mediated inhibition), activation of Rho A/ROCK, and neurite retraction. We hypothesize that the use of ibuprofen (a non-steroidal anti-inflammatory drug, NSAID, and Rho A inhibitor) and Y-2372 (a selective ROCK inhibitor) has the ability to enhance neurite outgrowth despite the presence of inhibitory Aβ. Demonstration of which acts as a validation step for the use of this *in vitro* model system as an assay to measure neurotoxicity and subsequently screen methods of recovery, acting as a pre-clinical tool that can help to streamline the drug development pipeline in a robust and quantifiable manner.

Methods

Cell culture: induction of neurite outgrowth from human pluripotent stem cells

Neurite outgrowth was induced from the embryonal carcinoma (EC) cell line, TERA2.cl.SP12, as previously described (Clarke et al., 2017). TERA2.cl.SP12 are well-established lineages derived from the original TERA2 population with a propensity to differentiate toward a neuronal lineage and provide well-characterized model neurons for use in neurite outgrowth studies, as previously described (Przyborski, 2001; Stewart et al., 2003; Przyborski et al., 2004; Gertow et al., 2007; Maltman et al., 2009). ReproNeuro iPSC-derived neuroprogenitor cells (Reprocell Europe Ltd., Glasgow, UK) were revived directly into an AggreWell™ 800 plate (STEMCELL Technologies, Cambridge, UK) to induce cellular aggregation. Neurospheres were then placed on two-dimensional (2D) (48-well tissue culture plate (Greiner Bio-One, Stonehouse, UK)) or three-dimensional (3D) (Alvetex® Scaffold (ReproCELL Europe Ltd.)) surfaces coated overnight in 10 µg/mL poly-D-lysine (Sigma-Aldrich, Irvine, UK) and laminin (Sigma-Aldrich) and cultured in the presence of mitotic inhibitors (1 µM cytosine arabinose (Sigma-Aldrich), 10 µM 5'fluoro 2'deoxyuridine (Sigma-Aldrich) and 10 µM uridine (Sigma-Aldrich)) for 10 days, during which time, neurites extended from the neurosphere mass. Throughout this 10-day neurite outgrowth phase, additives were included in the culture medium: 1 µM $A\beta_{40}$ (Sigma-Aldrich), 1 µM $A\beta_{42}$ (Tocris Bioscience, Bristol, UK), 1 µM Nogo-A extracellular peptide residues 1–40 (NEP1–40) (a competitive inhibitor of the NgR, Tocris Bioscience), 10 µM Y-27632 (ROCK inhibitor, Tocris Bioscience), and 100 µM ibuprofen (Sigma-Aldrich).

During the 10-day neurite outgrowth phase of culture, additives were introduced to the culture medium to assess their influence on neurite outgrowth. Subsequently, after the completion of the 10-day neurite outgrowth period, the cultures were immobilized in 4% paraformaldehyde for immunofluorescent analysis.

Test compounds ($A\beta_{40}$, $A\beta_{42}$, Y-27632, ibuprofen, and NEP1–40) were added to mature cultures during the neurite outgrowth phase of growth and not during the differentiation process, therefore, their impact on neurite growth specifically has been tested in this study, as opposed to their role in neuronal differentiation. $A\beta_{40}$ and $A\beta_{42}$ were added to the culture medium either alone, or in combinations ranging from 1:10–10:1, but totalling a concentration of 1 µM. Control cultures were treated with the same volume vehicle for comparison with each test compound, and in this case, the vehicle refers to phosphate buffer solution (PBS).

Alternatively, 2D growth substrates (48-well tissue culture plates) were coated with Aβ peptides ($A\beta_{40}$ and $A\beta_{42}$) prior to the seeding of neurospheres at a concentration range of 0.05–50 µg/mL overnight and were washed twice with PBS prior to neurosphere seeding.

Protein aggregation assay

The PROTEOSTAT® Protein Aggregation Assay (Enzo, Exeter, UK) was used to measure aggregation of Aβ peptides in culture medium as per manufacturer's instructions and analyzed using the Biotek Synergy H4 fluorescent plate reader

(ThermoFisher Scientific, Loughborough, UK) with excitation of 550 nm and emission of 600 nm.

Immunofluorescence analysis of two-dimensional and three-dimensional cultures

Both 2D and 3D neurite outgrowth models were immunostained for the pan-neuronal marker TUJ-1 expression (anti-β-III-tubulin, TUJ-1, ARG62683 (Cambridge Bioscience, Cambridge, UK)) and counterstained with Hoechst 33342 (Thermo Fisher Scientific) as previously described (Goncalves et al., 2023). Briefly, samples were permeabilized in 0.1% Triton X-100 (Sigma-Aldrich): 3D for 20 minutes and 2D for 10 minutes. 3D scaffolds were then blocked for 30 minutes, and 2D cultures were blocked for 60 minutes in a blocking solution consisting of 1% normal goat serum (Sigma-Aldrich) and 0.01% Tween (Sigma-Aldrich) in PBS. Cultures were incubated with the primary antibody diluted in blocking buffer for 1 (2D) or 2 (3D) hours at room temperature. Both 2D and 3D samples were then washed three times for 10 minutes in blocking buffer and incubated with the secondary antibody (Alexafluor® anti-rabbit 488 (Thermo Fisher Scientific) diluted in blocking buffer with the addition of the nuclear dye Hoechst 33342 (Thermo Fisher Scientific) for 1 hour at room temperature. Samples were then washed three times for 10 minutes in blocking buffer, and 3D scaffolds were mounted on microscope slides with Vectashield anti-fade mounting medium (Vector Laboratories, Peterbrough, UK), while 2D samples were stored in PBS prior to imaging. Samples were imaged using the Zeiss 880 confocal microscope with Zen software (Carl Zeiss, Cambridge, UK).

Image analysis

ImageJ IJ1.46r software (NIH, Bethesda, MD, USA) was used to quantify neurite outgrowth by tracing TUJ-1 positive neurites from 2D cultures and to measure neurite penetration through 3D scaffolds as previously described (Clarke et al., 2017; Goncalves et al., 2023). Briefly, for 2D cultures, a grid was superimposed over the image, and three squares were selected at random for quantification. Neurites that made contact with the neurosphere in these squares were quantified, and neurites were traced using the freehand line tool to produce measurements of length, number, and density. For 3D cultures, the multi-point tool was used to identify neurites from the underside of the scaffold; the total number of neurites that penetrated the scaffold was recorded in each case (Clarke et al., 2017).

Statistical analysis

GraphPad Prism v10 (GraphPad Software, San Diego, CA, USA, www.graphpad.com) was used to determine statistical significance and either a one-way or two-way analysis of variance (ANOVA) with Tukey's *post hoc* analysis was conducted as appropriate. Differences were considered significant at $P < 0.05$. In all cases, neurites from three neurospheres were measured across three independent replicates, in total 9 neurospheres for each experimental condition were quantified, with over 100 neurites measured from each neurosphere (Clarke et al., 2017; Goncalves et al., 2023). This sample size was consistent with a previous study and has been evaluated for statistical significance previously (Clarke et al., 2017).

Results

Exogenous amyloid-β inhibits neurite outgrowth *in vitro*

A previous study has demonstrated reduced neurite growth across Aβ-bound surfaces (Postuma et al., 2000). To test this in our EC cell-derived neuronal model system, we coated 2D culture substrates with a range of concentrations (0.05–50 μg/mL) of $A\beta_{40}$ or $A\beta_{42}$ and measured neurite outgrowth following 10 days (**Figure 1A**). TUJ-1 positive neurites radiated from the central neurosphere mass in all conditions (**Figure 1B**), with neurites visibly shorter and sparse at the highest concentration (50 μg/mL) for both peptides.

Quantification of neurite density (**Figure 1C**) confirms a dose-dependent decrease in neurite outgrowth with increasing concentrations of both $A\beta_{40}$ and $A\beta_{42}$, with fewer neurites present on $A\beta_{42}$-coated substrates. Neurite length (**Figure 1D**) was particularly reduced at the highest concentration of peptide coating (50 μg/mL) and with $A\beta_{42}$ coating as opposed to $A\beta_{40}$.

Although this data supports that of other studies described in the literature, in the brains of AD patients, neurites are not exposed to Aβ peptides in isolation but in combination, and the ratio of which is indicative of disease progression (Hansson et al., 2019). Therefore, we progressed to adding exogenous Aβ to the culture medium of neurospheres, either alone or in combination at a variety of ratios (**Figure 2A**). Similarly, neurite growth was identified (**Figure 2B**) as TUJ-1 positive neurites radiating from the central neurosphere mass.

The enhanced capacity of $A\beta_{42}$ to aggregate in this environment was confirmed through a protein aggregation assay (**Figure 2C**). Neurite density (**Figure 2D**) was significantly reduced both in the case of $A\beta_{40}$ ($P < 0.0001$) and $A\beta_{42}$ ($P < 0.0001$) in isolation compared with the vehicle control, but not significantly distinguishable from each other. Neurite length (**Figure 2E**) was also significantly reduced for both $A\beta_{40}$ ($P < 0.0001$) and $A\beta_{42}$ ($P < 0.0001$) treatments, but in this case, $A\beta_{42}$ treatment resulted in significantly shorter neurites than $A\beta_{40}$ treatment alone ($P < 0.0001$).

When applied in combination, all Aβ conditions resulted in significantly ($P < 0.01$) reduced neurite density compared with vehicle-matched controls (**Figure 2F**), however, the extent of the reduction varied. Whereas neurite length (**Figure 2G**) was significantly reduced in all Aβ conditions compared with the vehicle control and was further significantly ($P = 0.0001$) reduced in all combination treatments compared with either $A\beta_{40}$ or $A\beta_{42}$ alone. An $A\beta_{42/40}$ ratio of 1:10 is typical of a healthy brain (Näslund et al., 1994), whereas increasing $A\beta_{42/40}$ ratios of 5:1 and 10:1 are indicative of an AD phenotype and resulted in the shortest neurites measured.

Modulation of downstream Nogo signalling promotes neurite regrowth in two-dimensional and three-dimensional cultures

The glial scar is the inhibitory environment that arises post-spinal cord injury (SCI) and has been widely studied. It involves the activation of receptors, including the Nogo receptor (NgR), by inhibitory molecules released from damaged neurons, resulting in the perturbation of actin dynamics via Rho A and

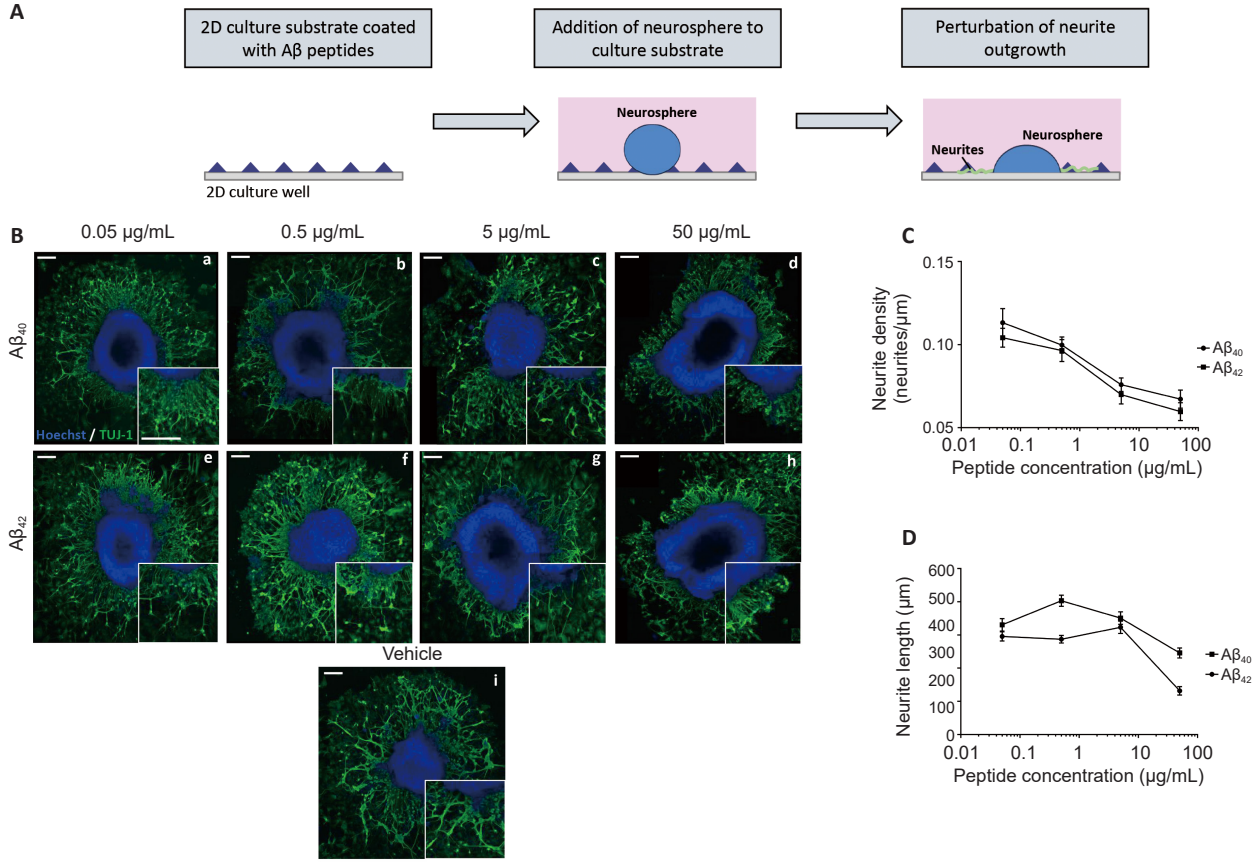

Figure 1 | **Substrate bound amyloid-β peptides inhibit neurite growth in a dose-dependent manner.**
Differentiated embryonal carcinoma cell-derived neurospheres were placed on 2D growth substrates coated with poly-D-lysine and laminin, supplemented with a range of concentrations (0.05–50 μg/mL) of amyloid-β, for 10 days prior to neurite observation (A). Immunofluorescence images (B) highlighting the pan-neuronal marker TUJ-1 (green) and cell nuclei (blue) demonstrate radiating neurite growth from the central neurosphere mass. Scale bars: 100 μm. A dose-dependent reduction in neurite density (C) (n = 9) was observed for both $A\beta_{40}$ and $A\beta_{42}$ peptides. Similarly, a reduction in neurite length (D) (n = 9) was observed at the highest concentrations tested. Data are presented as the mean ± SEM. Aβ: Amyloid-β.

ROCK, ultimately leading to growth cone collapse and neurite retraction (Schwab, 2010). It has been speculated that Aβ-mediated neurite inhibition may share commonalities with this pathway through the interaction of Aβ with NgR (Park and Strittmatter, 2007). To investigate this in 2D culture, we added a combination of 1 μM $A\beta_{40}$ with NgR pathway inhibitors to the culture medium of neurospheres during the 10-day neurite outgrowth period (**Figure 3A**). NEP1–40, a competitive inhibitor of the NgR, Y-27632, a ROCK inhibitor, and ibuprofen, which inhibits Rho A, were all used to elucidate the molecular mechanisms that underlie Aβ-mediated neurite inhibition.

Immunofluorescence analysis of TUJ-1 and nuclei reveals significant neurite outgrowth from samples (**Figure 3B**). Neurite density measurements (**Figure 3C**) reveal significantly reduced neurite outgrowth due to Aβ treatment (P < 0.0001). Restoration of neurite growth to levels that did not significantly differ from the vehicle-matched control was observed through NEP1–40 and Y-27632 treatments, and enhancement of neurite growth that significantly surpassed that of the vehicle control was achieved by ibuprofen treatment (P < 0.0001). Neurite length (**Figure 3D**), however, was significantly reduced in all conditions compared with the vehicle-matched control (P < 0.0001).

A 3D culture environment was also adopted to provide a more physiologically relevant geometry for developing neurites. This well-characterized model of neurite outgrowth has been applied in many previous studies, providing a robust, quantifiable assay (Clarke et al., 2017; Goncalves et al., 2023). Neurospheres were placed onto the 3D scaffold for the 10-day neurite outgrowth phase of culture, with the same combination of molecules added to the culture medium: Aβ alone or in combination with NEP1–40, ibuprofen, or Y-27632 (**Figure 4A**). Neurites were visualized as TUJ-1 positive protrusions visible from the underside of the scaffold (**Figure 4B**), having fully penetrated the material.

Neurite penetration (**Figure 4C**) was significantly reduced in the presence of Aβ alone (P = 0.0010), confirming 2D findings. However, neurite penetration was not restored by the addition of NEP1–40 and was still significantly reduced compared with controls (P = 0.0366). Ibuprofen treatment restored neurite penetration to a level that did not significantly differ from the vehicle control, whereas Y-27632 enhanced neurite penetration to a level that surpassed that of the control (P < 0.0001).

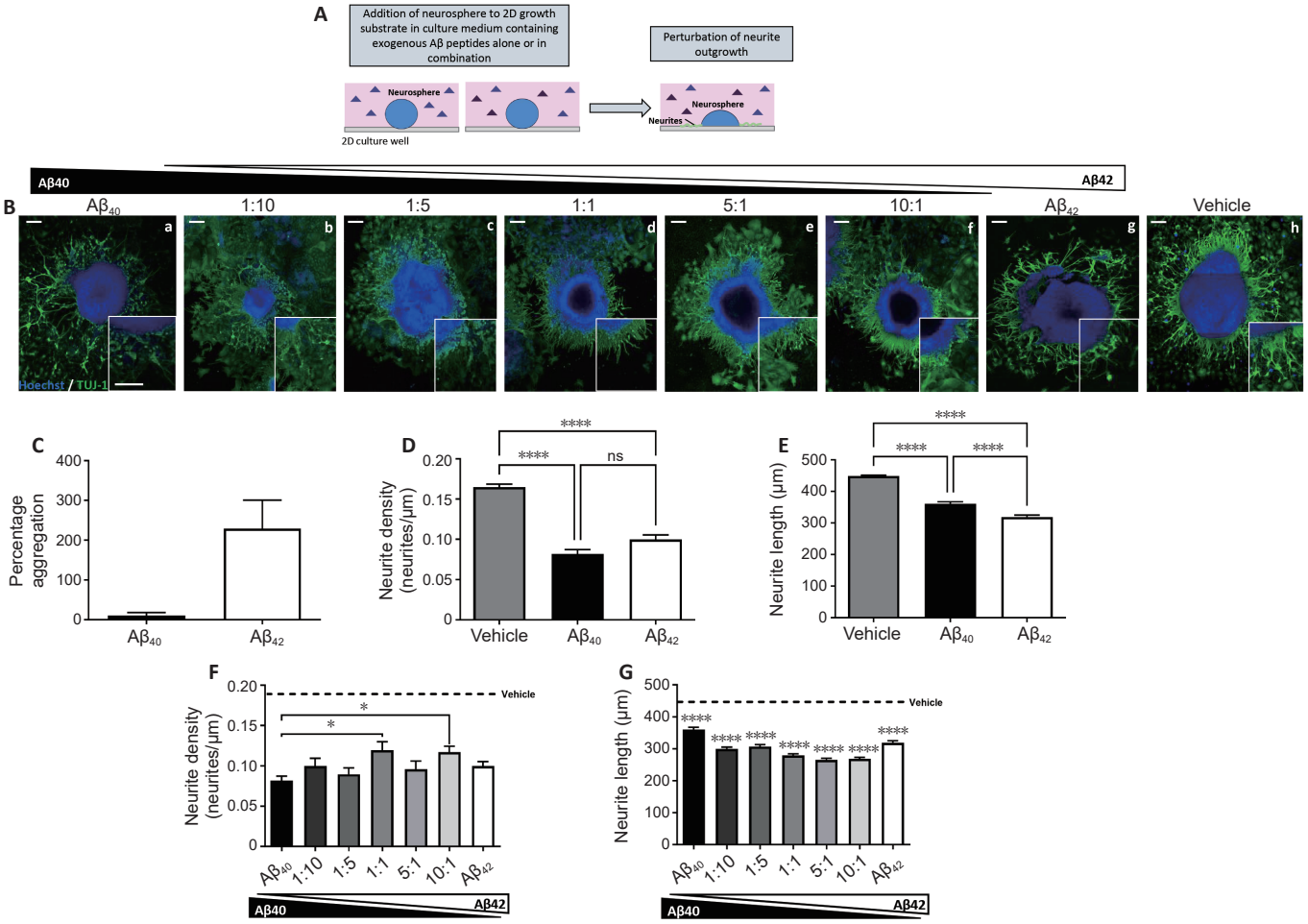

Figure 2 | **Exogenous Aβ reduces neurite outgrowth in physiologically relevant ratios.**
Embryonal carcinoma-derived neurospheres were placed on 2D growth substrates in culture medium containing 1 μM Aβ peptides for 10 days, prior to the visualization of neurite outgrowth (A). $Aβ_{40}$ and $Aβ_{42}$ were added alone or in combination, resulting in a final concentration of 1 μM. Immunofluorescence analysis (B) reveals TUJ-1-positive (green) neurites radiating from a central neurosphere mass (blue), with the extent of neurite outgrowth varying according to the treatment condition. Scale bars: 100 μm. The ability of $Aβ_{42}$ to aggregate more readily was confirmed through a protein aggregation assay and expressed as a percentage of aggregation (C) (n = 3). Neurite density (D) in the presence of $Aβ_{40}$ and $Aβ_{42}$ supplementation was significantly reduced compared with controls, but did not differ significantly from each other (n = 9, P < 0.0001). Neurite length (E) was significantly reduced with both $Aβ_{40}$ and $Aβ_{42}$ treatments (n = 9, P < 0.0001). Additionally, neurite density (F) was significantly reduced in the presence of combined Aβ treatments compared with the vehicle-matched control (dashed line) (n = 9, P < 0.0001). Furthermore, neurite length (G) was significantly reduced by all combined Aβ treatments compared with both the vehicle-matched control and either $Aβ_{40}$ or $Aβ_{42}$ alone (n = 9, P < 0.0001). *P < 0.05, ****P < 0.0001 (one-way analysis of variance with Tukey's *post hoc* test). Data are presented as the mean ± SEM. Aβ: Amyloid-β; ns: not significant.

Endogenous production of amyloid-β reduces neurite outgrowth which is restored by Rho A/ROCK inhibition

To further increase the complexity and physiological relevance of this assay system, we incorporated iPSC-derived neuroprogenitor cells that express an AD-associated mutation (PSEN1) and endogenously secrete an elevated $Aβ_{42/40}$ ratio. The same method was applied, whereby neurospheres were seeded onto 2D growth surfaces in the presence of an array of small molecules or drugs and cultured for 10 days to allow for neurite outgrowth (**Figure 5A**). Neurite growth from wild-type (WT) cells with (**Figure 5Bd–f**) and without (**Figure 5Ba–c**) exogenous $Aβ_{40}$ was observed, as well as in combination with ibuprofen (**Figure 5Be**) or Y-27632 (**Figure 5Bf**). Similarly, mutation cells were cultured without supplementation (**Figure 5Bg**) or supplemented with ibuprofen (**Figure 5Bh**) or Y-27632 (**Figure 5Bi**).

Neurite density (**Figure 5C**) was significantly reduced in WT cells exposed to exogenous Aβ40 (P < 0.0001) and mutation cells. Ibuprofen (P = 0.0038) and Y-27632 (P = 0.0046) significantly enhanced neurite outgrowth to a level comparable to WT in the presence of exogenous $Aβ_{40}$. Similarly, ibuprofen (P = 0.0038) and Y-27632 (P = 0.0046) treatment significantly enhanced neurite outgrowth from mutation cells to a similar level as WT. However, although neurite length (**Figure 5D**) was significantly reduced in WT with exogenous $Aβ_{40}$ (P = 0.0055), there was no significant difference between mutation and WT cells. Ibuprofen reduced neurite length in all conditions, significantly in the case of WT (P < 0.0001). However, Y-27632 had little effect on neurite length in WT cells with or without exogenous $Aβ_{40}$, but did significantly increase length in the case of mutation cells (P = 0.0377) compared with control cells.

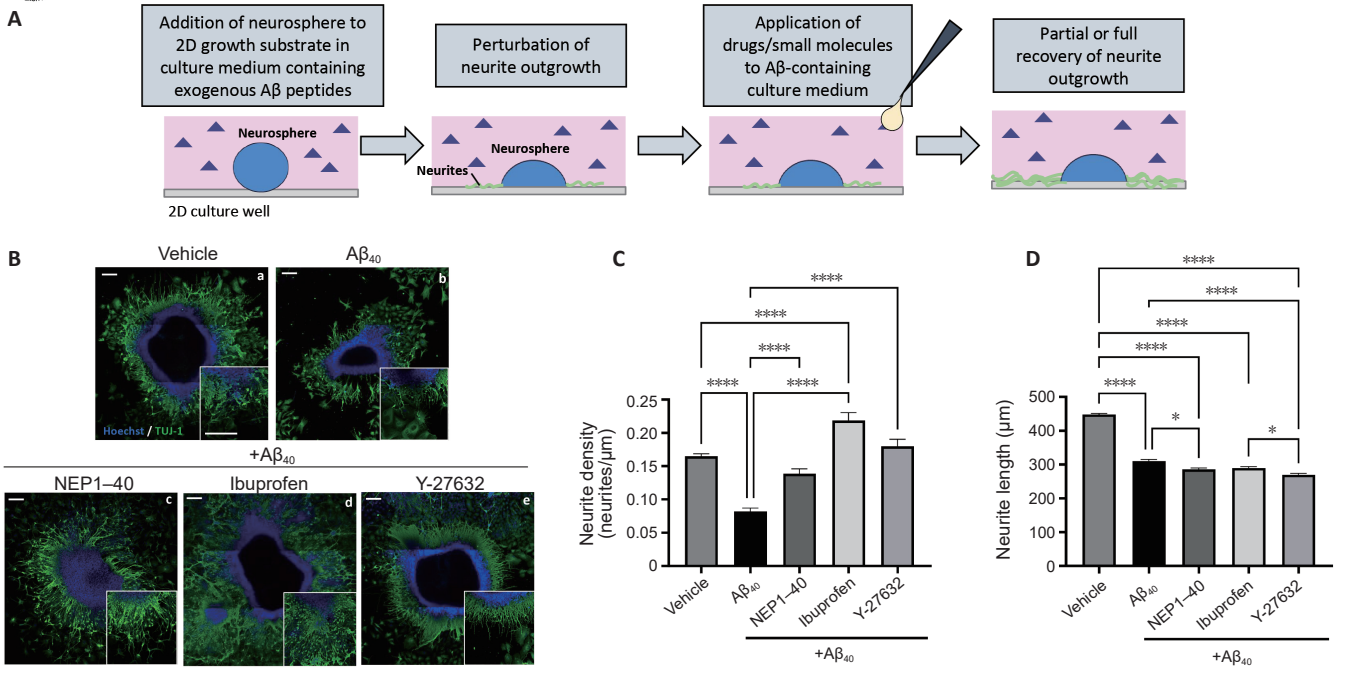

Figure 3 | **Modulation of NgR signalling restores neurite outgrowth in the presence of inhibitory $A\beta_{40}$.**
(A) Inhibitors targeting various aspects of NgR and its downstream signalling cascade were added to 2D cultures of embryonal carcinoma cell-derived neurospheres for a duration of 10 days, during which time neurites extended. Immunofluorescence analysis (B) utilizing the pan neuronal marker TUJ-1 (green) emphasized neurite outgrowth, while nuclei were stained with Hoechst (blue). Scale bars: 100 μm. Neurite density (C) was significantly reduced by $A\beta_{40}$ treatment compared with the vehicle-matched control. Both 1 μM NEP1–40 (NgR inhibitor) and 10 μM Y-27632 (ROCK inhibitor) restored neurite density to a level that did not significantly differ from the vehicle control. Conversely, 100 μM ibuprofen treatment significantly enhanced neurite density ($n = 9$, $P < 0.0001$). Neurite length (D) was significantly reduced by all treatment conditions compared with the vehicle-matched control ($n = 9$, $P < 0.0001$). $^*P < 0.05$, $^{****}P < 0.0001$ (one-way analysis of variance with Tukey's *post hoc* test). Data are presented as mean ± SEM. 2D: Two-dimensional; Aβ: amyloid-β.

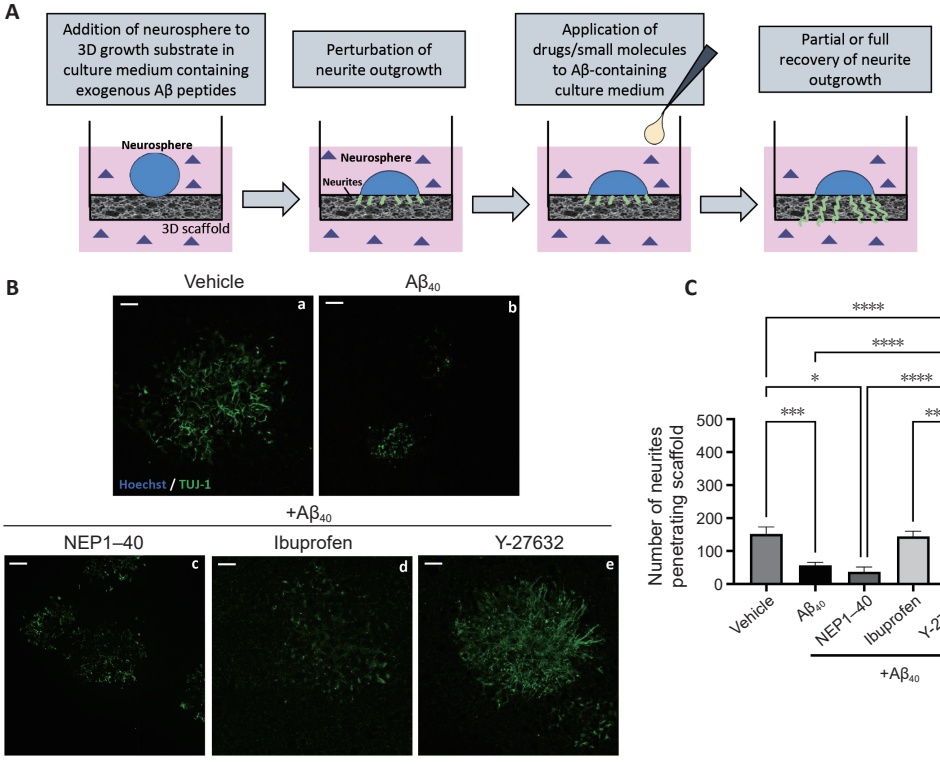

Figure 4 | **Modulation of Rho A/ROCK signalling attenuates $A\beta_{40}$-mediated neurite inhibition in 3D culture.**
Embryonal carcinoma cell-derived neurospheres were seeded onto 3D culture substrates in the presence of culture medium supplemented with 1 μM $A\beta_{40}$ alone or in combination with test compounds: 1 μM NEP1–40 (NgR inhibitor), 100 μM ibuprofen, or 10 μM Y-27632 (ROCK inhibitor; A). Neurite penetration was visualized as neuritic TUJ-1 positive (green) extensions from the underside of the scaffold (B). Scale bars: 100 μm. Quantification of neurite penetration (C) ($n = 9$) revealed a significant reduction in the presence of $A\beta_{40}$ alone ($P = 0.0010$) and in combination with NEP1–40 ($P = 0.0360$), whereas ibuprofen restored neurite penetration to control levels and Y-27632 significantly enhanced neurite penetration ($P < 0.0001$). $^*P < 0.05$, $^{***}P < 0.001$, $^{****}P < 0.0001$ (one-way analysis of variance with Tukey's *post hoc* test). Data are presented as mean ± SEM. 3D: Three-dimensional; Aβ: amyloid-β.

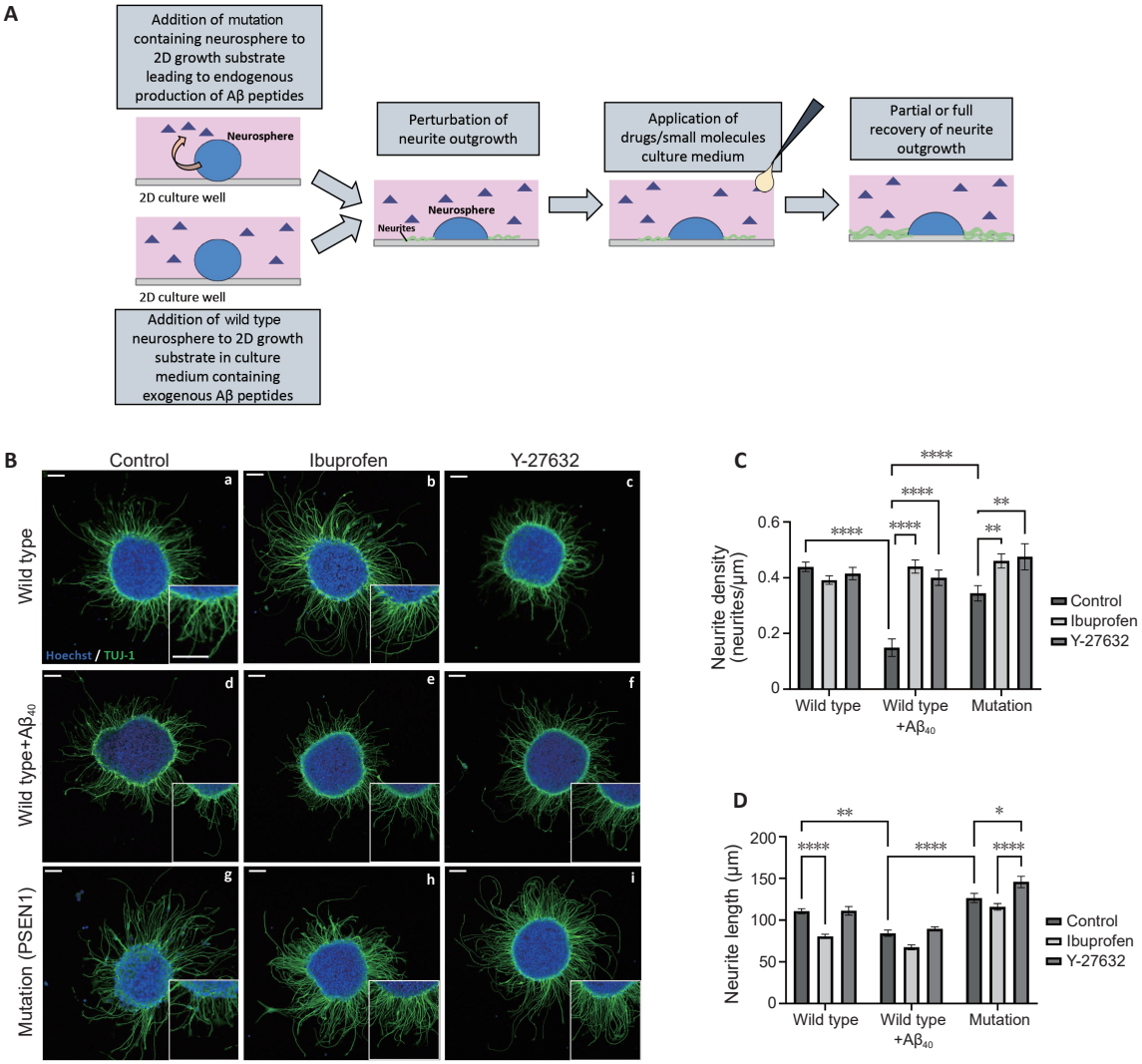

Figure 5 | Neurite outgrowth from neurospheres that possess AD-associated mutation is reduced and rescuable through Rho A/ROCK modulation in 2D culture.

Neurospheres were formed from induced pluripotent stem cell–derived neuroprogenitor cells from either wild-type (WT) or cells transfected with an AD-associated mutation in presenilin-1 (mutation) phenotypes. Neurospheres were seeded onto 2D culture substrates and treated with a range of medium supplementations: 1μM $A\beta_{40}$, 1 μM NEP1–40 (NgR inhibitor), 100 μM ibuprofen, or 10 μM Y-27632 (ROCK inhibitor) for 10 days prior to neurite outgrowth analysis (A). TUJ-1 positive (green) neurites radiate from a central neurospheres mass, where nuclei containing perikarya reside (blue) (B). Scale bars: 100 μm. Neurite density (C) (n = 9) was significantly reduced in WT cells supplemented with $A\beta_{40}$ ($P < 0.0001$), and both ibuprofen and Y-27632 treatments enhanced neurite density in WT + $A\beta_{40}$ and mutation-containing cells. Neurite length (D) (n = 9) was significantly reduced in the WT + $A\beta_{40}$ ($P = 0.0055$) condition and negatively affected by ibuprofen in all cases. *$P < 0.05$, ** $P < 0.01$, ****$P < 0.0001$ (two-way analysis of variance with Tukey's *post hoc* test). Data are presented as mean ± SEM. 2D: Two-dimensional; AD: Alzheimer's disease; Aβ: amyloid-β.

This study was then translated into a 3D environment more reminiscent of *in vivo* neurite development, by adding neurospheres derived from WT or mutation phenotype iPSCs onto a 3D culture substrate in the presence or absence of test compounds (**Figure 6A**). Neurite penetration from the underside of the scaffold was visualized as TUJ-1-positive neurites (**Figure 6B**). Quantification (**Figure 6C**) revealed significantly reduced neurite penetration in WT cells supplemented with $A\beta_{40}$ ($P = 0.0018$) and mutation-containing cells ($P = 0.0030$). Ibuprofen ($P = 0.0101$) and Y-27632 ($P = 0.0404$) significantly reduced neurite penetration in WT cells, but increased neurite penetration to a small degree in cells supplemented with $A\beta_{40}$ and mutation samples compared with respective controls.

Discussion

Loss of neuronal connectivity is one of the pathogenic mechanisms responsible for memory loss in AD (Citron, 2002; Rapoport et al., 2002; Mattson, 2004; Ittner and Gotz, 2011; Mokhtar et al., 2013; Cummings et al., 2014; Mangialasche et al., 2017). Many factors contribute to this loss of connectivity, one of which is the deposition of Aβ as senile plaques (Zheng et al., 2002; LaFerla et al., 2007; Gouras et al., 2015), leading to neuritic abnormalities that impede neuronal signal transmission (Knowles et al., 1999; Grutzendler et al., 2007). The ability of Aβ to induce neurite inhibition in simple culture systems has previously been demonstrated (Postuma et al., 2000; Petratos et al., 2008). However, the molecular intricacies that govern neurite inhibition in this context remain

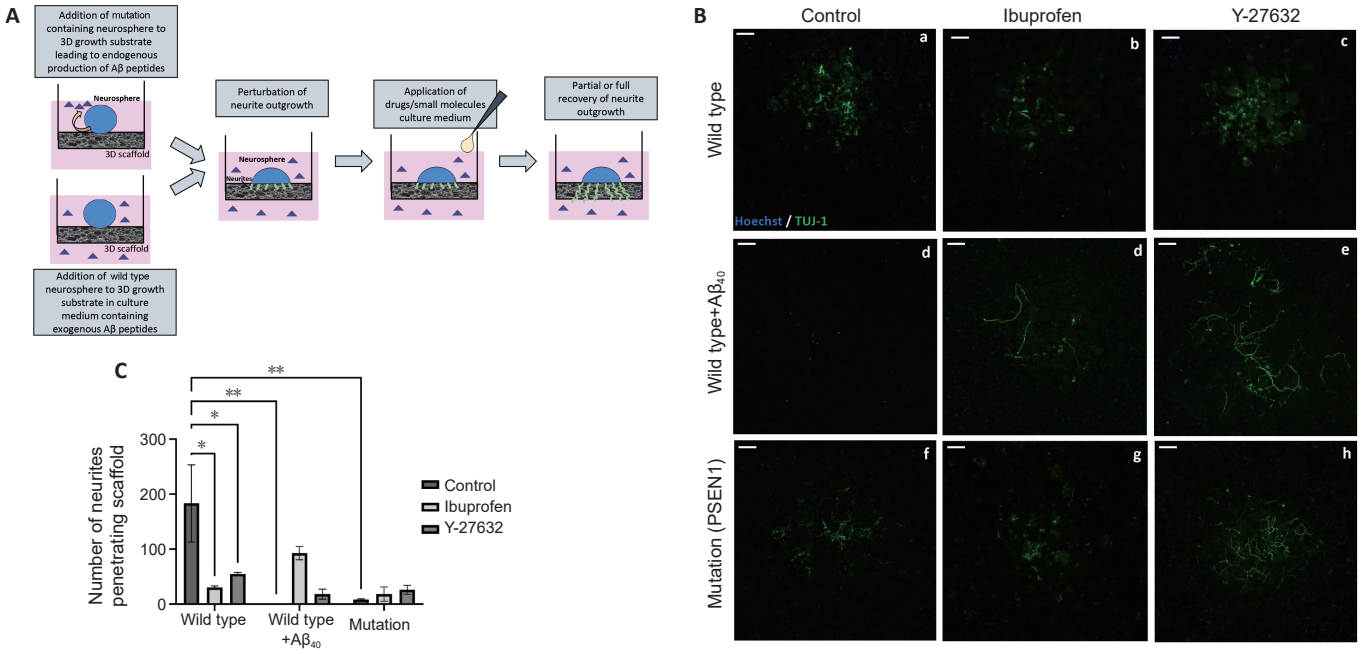

Figure 6 | **Neurite outgrowth in 3D is reduced from neurospheres that possess AD-associated mutation.**
Neurospheres comprised of induced pluripotent stem cell–derived neuroprogenitor cells were seeded onto 3D growth substrates with a combination of media additives: 1 μM $A\beta_{40}$, 1 μM NEP1–40 (NgR inhibitor), 100 μM ibuprofen, or 10 μM Y-27632 (ROCK inhibitor) for 10 days prior to neurite outgrowth analysis (A). Neurite penetration (TUJ-1, green) was visualized from the underside of the scaffold (B). Scale bars: 100 μm. (C) Quantification of neurite penetration (n = 9) revealed a significant reduction in both WT + $A\beta_{40}$ (P = 0.018) and mutation (P = 0.0030) containing samples. *P < 0.05, **P < 0.01 (two-way analysis of variance with Tukey's *post hoc* test). Data are presented as mean ± SEM. 3D: Three-dimensional; AD: Alzheimer's disease; Aβ: amyloid-β; WT: wide-type.

relatively unknown. Here, we describe that exogenous $A\beta_{40}$ and $A\beta_{42}$ are inhibitory to neurite outgrowth in a variety of ratios representative of disease progression, and attribute a reduction in neurite length to a rise in the ratio of $A\beta_{42}$ relative to $A\beta_{40}$, a hallmark of AD progression. Therefore, this indicates a potential mechanism linking a rise in $A\beta_{42}$ species in the brain of AD patients with reduced neuronal transmission.

Aβ interactions with the NgR have been speculated in the literature (Park et al., 2006; Zhou et al., 2011). NgR is one of the receptors that mediates neurite inhibition in the glial scar that arises post-SCI, and it acts through downstream Rho A and ROCK activation, leading to growth cone collapse. Here, we found partial but incomplete recovery of neurite inhibition through deactivation of NgR, with a restoration of neurite density but still a reduction in length in 2D samples. No effect was observed with 3D cultured samples, suggesting that although Aβ may induce neurite inhibition through NgR, it may be one of multiple pathways involved. This is also the case in molecular signaling post-SCI, as NgR is one of many receptors implicated in neurite inhibition in this context, with NgR2, NgR3, LAR, and PTPσ receptor complexes also involved in this response. Aβ-governed neurite inhibition may in part be mediated by NgR, but it may also involve additional receptor complexes, such as those involved in glial scar signaling, or even a novel receptor. However, in this study, we do provide evidence of partial involvement of NgR, along with strong evidence that the molecular pathways involved in Aβ-mediated inhibition are governed by Rho A/ROCK activation.

The ability of the selective ROCK inhibitor, Y-27632, to overcome Aβ-mediated inhibition has previously been documented in a simple SH-SY5Y model of neurite outgrowth (Postuma et al., 2000). This suggests that the Rho A/ROCK signalling pathway is involved in Aβ-induced neurite inhibition or potently induces neurite growth to a point that can overcome the deleterious effects of Aβ, similar to the signalling events that underlie inhibition following SCI (Fawcett and Asher, 1999; Monnier et al., 2003; Chan et al., 2005; Yiu and He, 2006; Lingor et al., 2007; Gopalakrishnan et al., 2008). In this study, we have further evidenced this, by demonstrating the ability of Y-27632 and ibuprofen, an inhibitor of Rho A known to enhance neurite outgrowth (Fu et al., 2007; Dill et al., 2010; Kopp et al., 2012; Roloff et al., 2015), to overcome neurite inhibition induced by exogenous and endogenously secreted Aβ in two model systems. Besides being an inhibitor of Rho A, ibuprofen is also a non-steroidal anti-inflammatory drug (NSAID) that inhibits prostaglandin synthesis, therefore its mechanism of neurotrophic action may also be a consequence of its anti-inflammatory properties, which is an avenue worthy of further investigation.

These data suggest that Aβ inhibition is mediated by Rho A/ROCK activation or that deactivation of Rho A/ROCK potently drives neurite initiation and extension to the point that it is able to overcome inhibitory stimuli such as Aβ. It also highlights the potential neural regeneration properties of Rho A/ROCK inhibitors, particularly as ibuprofen enhanced neurite outgrowth to greater than control levels in some of the conditions outlined within this study. The disparity observed between neurite density and length in several of the experimental conditions described suggests that neurite initiation and extension may be controlled by independent mechanisms, and warrants further investigation.

We also described a novel AD-specific model of neurite outgrowth that has many potential applications, including drug discovery and personalised medicine. Building on the development of several iPSC-derived AD-model neuroprogenitor cell lines, such as those described by Yagi et al. (2011), we developed a novel neurosphere-based neurite outgrowth assay. We demonstrated an application of this model to study neurite induction from cells transfected with an AD-associated mutation in presenilin 1 (PSEN1). The presenilins form the γ-secretase complex, which is involved in the proteolytic cleavage of amyloid precursor protein and the formation of Aβ species (Citron et al., 1997; Selkoe, 1998; Haapasalo and Kovacs, 2011; Yagi et al., 2011; Sproul et al., 2014). Due to this mutation, cells express a higher $A\beta_{42}$:$A\beta_{40}$ ratio, providing a more complex *in vitro* model that better recapitulates aspects of the *in vivo* diseased state.

We found that neurospheres derived from AD-model cells generated less dense neurite outgrowth than WT neurospheres, indicating impaired neurite generation. This effect was recovered by medium supplementation with Y-27632 and ibuprofen, further evidencing the role of Rho A and ROCK-mediated signalling in driving neurite growth.

In this study, we not only present a novel application for an established neurite outgrowth assay, but we also introduce the concept of disease-specific modifications to the existing methodology. Through the incorporation of iPSC-derived neuroprogenitor cells containing an AD-associated mutation, we have been able to demonstrate the ability to tailor this system to meet the needs of specific diseases where impaired neural connectivity is implicated as a pathogenic mechanism, such as Parkinson's disease (Takenouchi et al., 2001), schizophrenia (Miyoshi et al., 2003), and Down's syndrome (Murtomäki et al., 1992). This methodology also lends itself to other neurological diseases, and through iPSC technology and the proof-of-concept data described in this study, our model system offers a new assay to measure changes in neurite growth, development, and connectivity in a wide range of conditions. Incorporation of iPSC-derived neuroprogenitor cells also has implications in terms of personalized medicine, as patient-derived differentiated iPSCs could be incorporated into this model system, which in turn acts as a quantifiable assay to screen the efficacy and regenerative capacity of drugs in a patient-specific manner. Therefore, the data described in this study and the technology utilized have far-reaching impact on many aspects of the scientific community, including medical, industrial, and academic applications. Furthermore, it also provides a screening tool with the capacity to test a range of molecules for their ability to promote neurite regeneration. These proof-of-concept data demonstrate that neurite induction is robust and quantifiable from iPSC-derived neurospheres and can be applied to both personalized medicine modelling and disease-specific investigations.

Whilst this novel culture system offers a reductionist approach to determine the exact effects of Aβ on neurite outgrowth specifically, it is still a simplistic representation of the *in vivo* environment, which may be considered a limitation of the study. The brain is widely considered the most complex and poorly understood organ of the body, and Aβ deposition in senile plaques is one of multiple pathogenic mechanisms involved in AD progression. Whilst striving to recapitulate multiple aspects of AD-associated cellular interactions would help to improve the physiological relevance of the *in vitro* system, it would make it difficult to ascertain causative relationships. The inclusion of patient-derived cells, made possible by the iPSC-based strategy developed in this study, provides an opportunity to increase the complexity and physiological relevance of the system, whilst maintaining enough simplicity to draw clear conclusions.

In conclusion, our findings suggest that both Y-27632 and ibuprofen are potent inducers of neuritogenesis that can be used *in vitro* to overcome an inhibitory stimulus. We have also demonstrated the detrimental effects of exogenous Aβ species on neurite growth in human model neurites achieved through different methodologies, validating and strengthening the outcomes of the study. Moreover, we have demonstrated the ability of small molecule inhibition of Rho A and ROCK to overcome this inhibitory phenotype and promote neurite growth. The use of novel culture techniques, combining stem cell technologies and 3D cell culture, has provided a transformative platform for the investigation of neurite dynamics in the presence of both inhibitory and growth-inducing stimuli. Understanding the molecular mechanisms that underlie neurite dynamics in complex neurodegenerative diseases can help provide novel therapeutic targets that restore neural connectivity and provide a valuable *in vitro* preclinical platform. Furthermore, we also describe the development of a novel iPSC-based neurite outgrowth assay that has potential applications in the field of personalized medicine and drug discovery.

Author contributions: *KG and SP designed the study; KG performed the experiments, analyzed the data, wrote original draft; SP reviewed and edited original draft, obtained funding, and provided administrative and supervisory support. Both authors approved the final manuscript.*

Conflicts of interest: *SP is affiliated with the company Reprocell Europe Ltd. KG declares that there is no conflict of interest to disclose.*

Data availability statement: *No additional data are available.*

References

Cai Y, An SSA, Kim S (2015) Mutations in presenilin 2 and its implications in Alzheimer's disease and other dementia-associated disorders. Clin Interv Aging 10:1163-1172.

Chan CCM, Khodarahmi K, Liu J, Sutherland D, Oschipok LW, Steeves JD, Tetzlaff W (2005) Dose-dependent beneficial and detrimental effects of ROCK inhibitor Y27632 on axonal sprouting and functional recovery after rat spinal cord injury. Exp Neurol 196:352-364.

Citron M, et al. (1997) Mutant presenilins of Alzheimer's disease increase production of 42-residue amyloid [beta]-protein in both transfected cells and transgenic mice. Nat Med 3:67-72.

Citron M (2002) Alzheimer's disease: treatments in discovery and development. Nat Neurosci 5 Suppl:1055-1057.

Clarke KE, Tams DM, Henderson AP, Roger MF, Whiting A, Przyborski SA (2017) A robust and reproducible human pluripotent stem cell derived model of neurite outgrowth in a three-dimensional culture system and its application to study neurite inhibition. Neurochem Int 106:74-84.

Cummings JL, Morstorf T, Zhong K (2014) Alzheimer's disease drug-development pipeline: few candidates, frequent failures. Alzheimers Res Ther 6:37.

Dill J, Patel AR, Yang XL, Bachoo R, Powell CM, Li S (2010) A molecular mechanism for Ibuprofen-mediated RhoA inhibition in neurons. J Neurosci 30:963-972.
Dumurgier J, Gabelle A, Vercruysse O, Bombois S, Laplanche JL, Peoc'h K, Schraen S, Sablonnière B, Pasquier F, Touchon J, Lehmann S, Hugon J, Paquet C (2013) Exacerbated CSF abnormalities in younger patients with Alzheimer's disease. Neurobiol Dis 54:486-491.
Fawcett JW, Asher RA (1999) The glial scar and central nervous system repair. Brain Res Bull 49:377-391.
Fu Q, Hue J, Li S (2007) Nonsteroidal anti-inflammatory drugs promote axon regeneration via RhoA inhibition. J Neurosci 27:4154-4164.
Gertow K, Przyborski S, Loring JF, Auerbach JM, Epifano O, Otonkoski T, Damjanov I, Ahrlund-Richter L (2007) Isolation of human embryonic stem cell-derived teratomas for the assessment of pluripotency. Curr Protoc Stem Cell Biol Chapter 1:Unit1B.4.
Goncalves KE, Phillips S, Shah DSH, Athey D, Przyborski SA (2023) Application of biomimetic surfaces and 3D culture technology to study the role of extracellular matrix interactions in neurite outgrowth and inhibition. Biomater Adv 144:213204.
Gopalakrishnan SM, Teusch N, Imhof C, Bakker MHM, Schurdak M, Burns DJ, Warrior U (2008) Role of Rho kinase pathway in chondroitin sulfate proteoglycan-mediated inhibition of neurite outgrowth in PC12 cells. J Neurosci Res 86:2214-2226.
Gouras GK, Olsson TT, Hansson O (2015) β-amyloid peptides and amyloid plaques in Alzheimer's disease. Neurotherapeutics 12:3-11.
Grutzendler J, Helmin K, Tsai J, Gan WB (2007) Various dendritic abnormalities are associated with fibrillar amyloid deposits in Alzheimer's disease. Ann N Y Acad Sci 1097:30-39.
Haapasalo A, Kovacs DM (2011) The many substrates of presenilin/γ-secretase. J Alzheimer's Dis 25:3-28.
Hansson O, Lehmann S, Otto M, Zetterberg H, Lewczuk P (2019) Advantages and disadvantages of the use of the CSF Amyloid β (Aβ) 42/40 ratio in the diagnosis of Alzheimer's Disease. Alzheimers Res Ther 11:34.
Ittner LM, Gotz J (2011) Amyloid-beta and tau--a toxic pas de deux in Alzheimer's disease. Nat Rev Neurosci 12:65-72.
Jin M, Shepardson N, Yang T, Chen G, Walsh D, Selkoe DJ (2011) Soluble amyloid beta-protein dimers isolated from Alzheimer cortex directly induce Tau hyperphosphorylation and neuritic degeneration. Proc Natl Acad Sci U S A 108:5819-5824.
Knowles RB, Wyart C, Buldyrev S V, Cruz L, Urbanc B, Hasselmo ME, Stanley HE, Hyman BT (1999) Plaque-induced neurite abnormalities: Implications for disruption of neural networks in Alzheimer's disease. Proc Natl Acad Sci U S A 96:5274-5279.
Kopp MA, Liebscher T, Niedeggen A, Laufer S, Brommer B, Jungehulsing GJ, Strittmatter SM, Dirnagl U, Schwab JM (2012) Small-molecule-induced Rho-inhibition: NSAIDs after spinal cord injury. Cell Tissue Res 349:119-132.
Kumar A, Singh A, Ekavali (2015) A review on Alzheimer's disease pathophysiology and its management: an update. Pharmacol Rep 67:195-203.
LaFerla FM, Green KN, Oddo S (2007) Intracellular amyloid-beta in Alzheimer's disease. Nat Rev Neurosci 8:499-509.
Lingor P, Teusch N, Schwarz K, Mueller R, Mack H, Bahr M, Mueller BK (2007) Inhibition of Rho kinase (ROCK) increases neurite outgrowth on chondroitin sulphate proteoglycan in vitro and axonal regeneration in the adult optic nerve in vivo. J Neurochem 103:181-189.
Maltman DJ, Christie VB, Collings JC, Barnard JH, Fenyk S, Marder TB, Whiting A, Przyborski SA (2009) Proteomic profiling of the stem cellresponse to retinoic acid and synthetic retinoid analogues: identification of major retinoid-inducible proteins. Mol Biosyst 5:458-471.
Mangialasche F, Solomon A, Winblad B, Mecocci P, Kivipelto M (2017) Alzheimer's disease: clinical trials and drug development. Lancet Neurol 9:702-716.
Mattson MP (2004) Pathways towards and away from Alzheimer's disease. Nature 430:631-639.
Miyoshi K, Honda A, Baba K, Taniguchi M, Oono K, Fujita T, Kuroda S, Katayama T, Tohyama M (2003) Disrupted-In-Schizophrenia 1, a candidate gene for schizophrenia, participates in neurite outgrowth. Mol Psychiatry 8:685-694.
Mokhtar SH, Bakhuraysah MM, Cram DS, Petratos S (2013) The beta-amyloid protein of Alzheimer's disease: communication breakdown by modifying the neuronal cytoskeleton. Int J Alzheimers Dis 2013:910502.
Monnier PP, Sierra A, Schwab JM, Henke-Fahle S, Mueller BK (2003) The Rho/ROCK pathway mediates neurite growth-inhibitory activity associated with the chondroitin sulfate proteoglycans of the CNS glial scar. Mol Cell Neurosci 22:319-330.
Murphy MP, LeVine H 3rd (2010) Alzheimer's disease and the amyloid-beta peptide. J Alzheimers Dis 19:311-323.
Murtomäki S, Risteli J, Risteli L, Koivisto U-M, Johansson S, Liesi P (1992) Laminin and its neurite outgrowth-promoting domain in the brain in Alzheimer's disease and Down's syndrome patients. J Neurosci Res 32:261-273.
Näslund J, Schierhorn A, Hellman U, Lannfelt L, Roses AD, Tjernberg LO, Silberring J, Gandy SE, Winblad B, Greengard P, et al. (1994) Relative abundance of Alzheimer A beta amyloid peptide variants in Alzheimer disease and normal aging. Proc Natl Acad Sci U S A 91:8378-8382.
Park JH, Widi GA, Gimbel DA, Harel NY, Lee DHS, Strittmatter SM (2006) Subcutaneous Nogo receptor removes brain amyloid-β and improves spatial memory in Alzheimer's transgenic mice. J Neurosci 26:13279-13286.
Park JH, Strittmatter SM (2007) Nogo receptor interacts with brain APP and Aβ to reduce pathologic changes in Alzheimer's transgenic mice. Curr Alzheimer Res 4:568-570.
Petratos S, Li QX, George AJ, Hou X, Kerr ML, Unabia SE, Hatzinisiriou I, Maksel D, Aguilar MI, Small DH (2008) The beta-amyloid protein of Alzheimer's disease increases neuronal CRMP-2 phosphorylation by a Rho-GTP mechanism. Brain 131:90-108.
Postuma RB, He W, Nunan J, Beyreuther K, Masters CL, Barrow CJ, Small DH (2000) Substrate-bound β-amyloid peptides inhibit cell adhesion and neurite outgrowth in primary neuronal cultures. J Neurochem 74:1122-1130.
Przyborski SA (2001) Isolation of human embryonal carcinoma stem cells by immunomagnetic sorting. Stem Cells 19:500-504.
Przyborski SA, Christie VB, Hayman MW, Stewart R, Horrocks GM (2004) Human embryonal carcinoma stem cells: models of embryonic development in humans. Stem Cells Dev 13:400-408.
Rapoport M, Dawson HN, Binder LI, Vitek MP, Ferreira A (2002) Tau is essential to beta-amyloid-induced neurotoxicity. Proc Natl Acad Sci U S A 99:6364-6369.
Roloff F, Scheiblich H, Dewitz C, Dempewolf S, Stern M, Bicker G (2015) Enhanced neurite outgrowth of human model (NT2) neurons by small-molecule inhibitors of Rho/ROCK signaling. PLoS One 10:e0118536.
Sadigh-Eteghad S, Sabermarouf B, Majdi A, Talebi M, Farhoudi M, Mahmoudi J (2015) Amyloid-beta: a crucial factor in Alzheimer's disease. Med Princ Pract 24:1-10.
Schwab ME (2010) Functions of Nogo proteins and their receptors in the nervous system. Nat Rev Neurosci 11:799-811.
Serrano-Pozo A, Frosch MP, Masliah E, Hyman BT (2011) Neuropathological alterations in Alzheimer disease. Cold Spring Harb Perspect Med 1:a006189.
Selkoe DJ (1998) The cell biology of β-amyloid precursor protein and presenilin in Alzheimer's disease. Trends Cell Biol 8:447-453.
Spies PE, Slats D, Sjögren JM, Kremer BP, Verhey FR, Rikkert MG, Verbeek MM (2010) The cerebrospinal fluid amyloid beta42/40 ratio in the differentiation of Alzheimer's disease from non-Alzheimer's dementia. Curr Alzheimer Res 7:470-476.
Sproul AA, Jacob S, Pre D, Kim SH, Nestor MW, Navarro-Sobrino M, Santa-Maria I, Zimmer M, Aubry S, Steele JW, Kahler DJ, Dranovsky A, Arancio O, Crary JF, Gandy S, Noggle SA (2014) Characterization and molecular profiling of PSEN1 familial Alzheimer's disease iPSC-derived neural progenitors. PLoS One 9:e84547.
Stewart R, Christie VB, Przyborski SA (2003) Manipulation of human pluripotent embryonal carcinoma stem cells and the development of neural subtypes. Stem Cells 21:248-256.
Takenouchi T, Hashimoto M, Hsu LJ, Mackowski B, Rockenstein E, Mallory M, Masliah E (2001) Reduced neuritic outgrowth and cell adhesion in neuronal cells transfected with human alpha-synuclein. Mol Cell Neurosci 17:141-150.
Yagi T, Ito D, Okada Y, Akamatsu W, Nihei Y, Yoshizaki T, Yamanaka S, Okano H, Suzuki N (2011) Modeling familial Alzheimer's disease with induced pluripotent stem cells. Hum Mol Genet 20:4530-4539.
Yiu G, He Z (2006) Glial inhibition of CNS axon regeneration. Nat Rev Neurosci 7:617-627.
Zhang YW, Thompson R, Zhang H, Xu H (2011) APP processing in Alzheimer's disease. Mol Brain 4:3.
Zheng WH, Bastianetto S, Mennicken F, Ma W, Kar S (2002) Amyloid β peptide induces tau phosphorylation and loss of cholinergic neurons in rat primary septal cultures. Neuroscience 115:201-211.
Zhou X, Hu X, He W, Tang X, Shi Q, Zhang Z, Yan R (2011) Interaction between amyloid precursor protein and Nogo receptors regulates amyloid deposition. FASEB J 25:3146-3156.

C-Editor: Zhao M; S-Editor: Li CH; L-Editor: Song LP; T-Editor: Jia Y